Advances in Applied Mathematics and Mechanics
Adv. Appl. Math. Mech., Vol. **15**, No. 1, pp. 244-266

DOI: 10.4208/aamm.OA-2020-0108
February 2023

A Micro-Structure Dependent Buckling Analysis of Partially-Cracked Generally Orthotropic Plate under Thermal Domain

Ankur Gupta*, Shashank Soni and N. K. Jain

Department of Mechanical Engineering, National Institute of Technology, Raipur, Chhattisgarh 492010, India

Received 22 April 2020; Accepted (in revised version) 9 March 2021

Abstract. In this work, a non-classical analytical approach for buckling analysis of partially cracked generally orthotropic plate is proposed under the thermal domain. The derivation for the governing equation is based on the non-classical approach using Kirchhoff's thin plate theory and the modified couple stress theory. The effect of fibre orientation on critical buckling temperature is incorporated by considering the coefficients of mutual influence. Line spring model is applied with some modifications to formulate all the crack terms while the thermal effects are introduced in form of thermal in-plane moments and forces. The final governing equation is solved using Galerkin's method and the relation for critical buckling temperature as affected by fibre orientation is obtained. The variation of critical buckling temperature as affected by fibre orientation for different values of crack length, crack location and length scale parameter is presented. Also, the effect of fibre orientation on fundamental frequency under the thermal domain is analysed.

AMS subject classifications: 74K20

Key words: Orthotropic plate, fibre orientation, crack, microstructure, thermal domain.

1 Introduction

The orthotropic plate being an elementary structural unit is vastly used to obtain desired mechanical properties, especially in automobile, aerospace and naval applications. The application of orthotropic materials in micro-sized structure is evident from the literature [5, 11, 45]. It is seen that as the dimensions of general structures such as plates and shells reduce, the mechanical properties of such a micro-sized structure becomes size-dependent. For example, classical theories like Kirchhoff's thin plate theory and classical

*Corresponding author.
Emails: ankurgupta1729@gmail.com (A. Gupta), shashanksoninitr@gmail.com (S. Soni), nkjain.me@nitrr.ac.in (N. K. Jain)

shell theory underpredict the stiffness of micro-sized plates and shells. The micro-sized plates find their usage in various engineering applications such as micro-resonators, sensors and actuators, atomic force microscopes (AFMs), and micro-switches etc. At various instances, these micro-sized structures have to operate under the thermal domain which affects their stability, as well as mechanical properties, e.g. micro-sized computer elements in the form of plates and shells, are operated at wide range of temperature. Owing to its wide application, the mechanical properties of micro-sized structures has to be accurately determined including the external factor such as temperature or flaws in the form of cracks and holes.

In literature, it has been also observed that the presence of defects in form of cracks or holes in these structural units makes the dynamic behaviour severely different from that of an intact plate. Mostly numerical techniques are used for static solutions for the cracked plate, but an approximate analytical approach has been presented employing the simplified Line Spring Model (LSM). This model (LSM) was firstly proposed by Rice and Levy [37] and their concept of the line spring model was based on Kirchhoff's classical plate theory. They developed the line spring model for cracked plate considering bending and stretching compliances to determine the stress intensity factors at crack tips. King [29] established a pair of linear algebraic equations to analyze parameters of fracture by doing simplification of integral equations of LSM given in [37]. Later, Zeng and Dai [38] used this model [29] and calculated the stress intensity factors of a plate having angled surface crack subjected to a biaxial state of stresses. Bose and Mohanty [6] developed a model for vibration problems of a cracked thin isotropic plate having arbitrary crack position and orientation of crack and concluded that the crack orientation affects the frequency of the plate. Stahl and Keer [44] used the Fredholm integral equation of the second kind to investigate the natural frequency of the plate containing a centrally located internal crack and a side crack. Recently Xu et al. [49] have established an accurate and efficient solution method for free vibration and buckling of cracked NFRC rectangular thin plate using a symplectic approach and the line spring model. In their work, they concluded that both length and crack location are important factors that affect the vibration response and hygrothermal ageing of NFRC plates.

Solecki [39] analyzed the flexural vibration of a plate having an arbitrarily located crack for simply supported boundary condition by using the Fourier transformation functions and green gauss theorem. Liew et al. [31] has given the frequency response of cracked plates by employing the virtual principle with the Ritz method. Khadem and Rezaee [23] given a technique to detect the crack using modified comparison functions in a simply supported plate. The deviation of frequencies of a rectangular plate with arbitrary orientation of narrow slits is experimentally performed by Maruyama and Ichinomiya [47]. Using the application of the Ritz method Huang et al. [13] developed the new function for vibration response of plate with through internal crack of various orientations. Wu and Law [48] found that if the orientation of the crack is changed then it affects the vibration response of the plate having a moderate thickness. Jha et al. [20] thoroughly reviewed the literature on FGM plate and performed stability and dynamic

analysis of functionally graded plates. Israr et al. [15, 16] have proposed an analytical approach for analysis of an isotropic plate having a part-through crack parallel to one of its edges and gave approximate analytical results for vibrations characteristics. Their results show the decreasing effect of crack length on the frequency response of the plate. Extending this further, Ismail and Cartmell [14] presented results for a plate with a variably angled crack.

Jeyaraj et al. [19] used ANSYS and SYSNOISE to study the sonic response and vibration in isotropic plate subjected to an increase in temperature. Further, they also extended this work for composite plates [18]. Natarajan et al. [34] used FSDTA and performed a parametric study on vibration and thermal buckling of FGM plate considering a through internal crack. Jalaei and Civalek [17] studied the dynamic instability of embedded viscoelastic porous FG nanobeams under axially oscillating loading and magnetic field based on the Kelvin-Voigt model. Gupta et al. [9, 11] used MCST in combination with CPT to present frequencies of cracked micro-plates. In their work, they also showed the effect of fibre-orientation and microstructure on vibrations of cracked specially orthotropic micro plate [10]. Joshi et al. [23, 25] developed the analytical models to obtain vibration characteristics of thin isotropic and orthotropic lamina containing two cross (perpendicular) internal as well as surface cracks located at the centre. Further extending their work, they studied the buckling response of cracked thin isotropic [26] and specially orthotropic [24] plates subjected to an increase in temperature. Soni et al. [40–42] presented an analytical model to show the effect of surrounding fluidic medium on vibration characteristics of partially cracked isotropic [40], orthotropic [42] and MEE [42] plates.

For reliable design, it becomes interesting to study the impact of temperature on plate structures when it contains flaws such as cracks or holes. In the literature, a lot of researchers have put importance on vibration analysis of plates under thermal effects. Murphy et al. [33] worked out thermal buckling of clamped rectangular plates both theoretically and experimentally. The effect of temperature rise, volume fraction, edge conditions on vibration parameters of FGM plates has been studied by Yang and Shen [50] using higher-order theory. Li et al. [30] employed the 3D theory of elasticity whereas, Kim [28] considered third-order shear deformation to model thermal heating of FGM plate vibration.

Both, analytically and experimentally it has been established that the microstructure affects the stiffening of the plate and thus changes the vibration characteristics [32, 51]. Mindlin and Eshel [32] proposed a single internal length scale parameter to capture the size-effect of the plate. Papargyri-Beskou and Beskos [36] derived the governing equation of motion of gradient elastic flexural Kirchhoff plates, including the effect of in-plane constant forces on bending and presented a 6th order equation of gradient elasticity for a plate. To capture the microstructure effect in their study on the bending of a thin rectangular plate Mousavi and Paavola [35] considered two internal length scale parameters.

A novel mathematical equation for micro-plate employing the modified couple stress theory (MCST) is developed by Tsiatas [46]. Applying the model developed by Tsi-

atas [46] and Yin et al. [51] showed that the fundamental frequencies obtained from MCST are higher as compared to the Classical approach. Gao and Zhang [8] proposed a non-classical Kirchhoff plate model incorporating microstructure, surface energy and foundation effect and concluded that the presence of the elastic foundation reduces the plate deflection and increases the plate natural frequency. Akgöz and Civalek [1] have investigated the vibration response of non-homogenous and non-uniform microbeams in conjunction with Bernoulli-Euler beam and modified couple stress theory. Extending their work they have also presented the analytical solutions for bending, vibration and buckling problems of micro-sized plates based on modified couple stress theory [2] and modified strain gradient theory [3]. In their work they performed a detailed parametric study to demonstrate the effect of length scale parameter, length-to-thickness ratio on buckling load, deflection, and fundamental frequencies of micro plates. Based on Euler Bernoulli's beam theory Akgöz and Civalek [4] also have investigated the buckling and bending behavior of micro beams for various types of boundary conditions. They [4] studied the effects of additional material length scale parameters, material property variation function and slenderness ratio on the buckling response of FGM micro beams and also compared the results for different non-classical theories.

The literature [23–26] shows that the buckling behaviour of plates is affected by the presence of crack which is further influenced if the plate is functioning under the thermal domain. In the case of the orthotropic plate, the work of researchers [11,43] show that the stiffness of the plate is affected by the orientation of the fibres and length scale parameter. As per the author's knowledge, there has been no work reported in the literature where researchers have attempted to analytically obtain the critical buckling temperature as affected by the fibre orientation. The reason behind the lack of results may be due to the difficulty in the coupling of the shear and normal stresses for fibre orientation under the thermal domain. Thus, the study of the influence of crack and fibre orientation on the buckling behaviour of orthotropic plates with thermal effects becomes significant and therefore the present study proposes a new analytical model which addresses the following: 1. Buckling analysis of partially cracked orthotropic plate considering the effect of fibre orientations using non-classical analytical modelling. 2. A unique relation for critical buckling temperature (Tbcr) of cracked orthotropic micro-plate is derived considering the effect of fibre orientations. 3. The coupling effect of the shear and normal stresses using coefficients of mutual influence under the thermal domain has been incorporated in the constitutive relations. 4. The effect of temperature rise, fibre orientation, crack length, crack location and length scale parameter, on fundamental frequency and critical buckling temperature of the cracked orthotropic plate is studied under the thermal domain for two boundary conditions. 5. Graphical results are presented to show the effect of the length scale parameter on critical buckling temperature as affected by the reduction in plate dimensions.

The plate under investigation is shown in Fig. 1. Linear dimensions along x and y directions are L_1 and L_2, the plate thickness is h and the length of the crack is $2a$. The depth of the crack is kept constant throughout the work. The location of the crack is

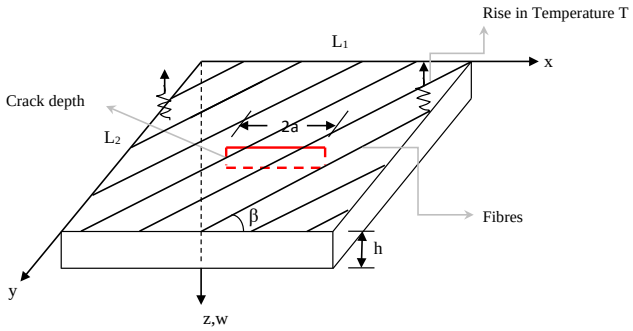

Figure 1: Fibrous Orthotropic plate containing a partial crack of length $2a$.

varied within the center line of the plate and parallel to the x-axis. β is the angle of fibres with one of the edges of the plate. Since, the plate under consideration is thin, hence the thickness of the plate h is much small as compared to the other two dimensions. Different values of internal material length scale parameter l are considered to compare the classical and non-classical results in the case of micro-plate.

2 Governing equation

The equation of motion which governs the linear vibration of an orthotropic rectangular plate with a part-through surface crack is derived using the equilibrium principle. It is considered that the crack is in the form of a continuous line. The modeling is subjected to the following assumptions:

1. The plate is assumed to be elastic, homogenous and the plate material is isotropic.

2. The plate has a uniform thickness h, which is very small as compared to its in-plane dimensions and all strain components follow Hooke's law.

3. The normal stress acting in the transverse direction of the plate is considered to be small and is neglected in the stress-strain relations.

4. It is assumed that the plane section normal to the middle surface will remain plane and normal to that surface before and after deformation. Hence the shear deformation is neglected.

5. The cracks terms are formulated using the line spring model and the phenomenon of crack opening or closing is neglected.

6. Effects of Rotary inertia and shear deformation are neglected.

The governing equation of a cracked orthotropic rectangular plate under influence of the thermal environment and based on approach of classical plate theory has been rigorously treated in [24] and can be stated as;

$$\begin{aligned}&D_x\frac{\partial^4 w}{\partial x^4}+2B\frac{\partial^4 w}{\partial x^2\partial y^2}+D_y\frac{\partial^4 w}{\partial y^4}\\&=-\rho h\frac{\partial^2 w}{\partial t^2}+\frac{\partial^2 m_y}{\partial y^2}+\frac{\partial^2 M_{Tx}}{\partial x^2}+\frac{\partial^2 M_{Ty}}{\partial y^2}-N_{Tx}\frac{\partial^2 w}{\partial x^2}-N_{Ty}\frac{\partial^2 w}{\partial y^2}+\frac{\partial^2 m_y}{\partial y^2}-n_y\frac{\partial^2 w}{\partial y^2}+P_z.\end{aligned}\tag{2.1}$$

Where,

$$D_x=\frac{E_x h^3}{12\left(1-\vartheta_x\vartheta_y\right)},\quad D_y=\frac{E_y h^3}{12\left(1-\vartheta_x\vartheta_y\right)}\quad\text{and}\quad D_t=G_{xy}\frac{h^3}{12}$$

represents the flexural and torsional rigidities respectively,

$$B=\frac{1}{2}\left(\vartheta_y D_x+\vartheta_x D_y+4D_t\right)$$

is the effective torsional rigidity. E_x, E_y, G_{xy}, ϑ_x and ϑ_y are the elastic constants. P_z is the lateral load, w is transverse deflection, ρ and h are the density and thickness of the orthotropic plate. M_{Tx}, M_{Ty} and N_{Tx}, N_{Ty} are the bending moment and in-plane compressive forces due to the thermal environment. m_y and n_y are the moment and force due to line crack.

Similarly, following the force and moment equilibrium principle and considering the extra force and moments due to the inclusion of the cracks and thermal environment, the governing equation of the cracked orthotropic plate with various fibre orientations is stated in the work of Soni et al. [43] as

$$\begin{aligned}&\frac{-\left(D_x+D^{Lx}\right)\left\{\left(\frac{\partial^4 w}{\partial x^4}+\vartheta_y\frac{\partial^4 w}{\partial x^2\partial y^2}\right)+\frac{\left(\vartheta_y m_y+m_x\right)}{\frac{1}{G_{xy}}-m_y^2E_y}\left(2\frac{\partial^4 w}{\partial x^3\partial y}+m_yE_y\frac{\partial^4 w}{\partial x^2\partial y^2}\right)\right\}}{1-\frac{E_x\left(\vartheta_y m_y+m_x\right)}{\left(1-\vartheta_x\vartheta_y\right)\left(\frac{1}{G_{xy}}-m_y^2E_y\right)}\left(m_x+m_y\vartheta_x\frac{E_y}{E_x}\right)}\\&+\frac{-2\left\{\begin{array}{c}\frac{h^3}{6}\frac{\partial^4 w}{\partial x^2\partial y^2}+\left(\left(D_x+D^{lx}\right)m_x+\vartheta_x\left(D_y+D^{ly}\right)m_y\right)\frac{\partial^4 w}{\partial x^3\partial y}+\Big\}\\\left(\left(D_y+D^{ly}\right)m_y+\vartheta_y\left(D_x+D^{lx}\right)m_x\right)\frac{\partial^4 w}{\partial y^3\partial x}\end{array}\right.}{\frac{1}{G_{xy}}-\frac{m_xE_x\left(\vartheta_y m_y+m_x\right)+m_yE_y\left(\vartheta_x m_x+m_y\right)}{\left(1-\vartheta_x\vartheta_y\right)}}\\&+\frac{-\left(D_y+D^{ly}\right)\left\{\left(\frac{\partial^4 w}{\partial y^4}+\vartheta_x\frac{\partial^4 w}{\partial x^2\partial y^2}\right)+\frac{\left(\vartheta_x m_x+m_y\right)}{\frac{1}{G_{xy}}-m_x^2E_x}\left(2\frac{\partial^4 w}{\partial y^3\partial x}+m_xE_x\frac{\partial^4 w}{\partial x^2\partial y^2}\right)\right\}}{1-\frac{E_y\left(\vartheta_x m_x+m_y\right)}{\left(1-\vartheta_x\vartheta_y\right)\left(\frac{1}{G_{xy}}-m_x^2E_x\right)}\left(m_y+m_x\vartheta_y\frac{E_x}{E_y}\right)}\\&=-\rho h\frac{\partial^2 w}{\partial t^2}-\frac{\partial^2 M_{Tx}}{\partial x^2}-\frac{\partial^2 M_{Ty}}{\partial y^2}-\frac{\partial^2 M_{Txy}}{\partial x\partial y}+\frac{\partial^2 m_y}{\partial y^2}-N_{Tx}\frac{\partial^2 w}{\partial x^2}\\&\quad-N_{Ty}\frac{\partial^2 w}{\partial y^2}-2N_{Txy}\frac{\partial^2 w}{\partial x\partial y}-n_y\frac{\partial^2 w}{\partial y^2}+P_z\end{aligned}\tag{2.2}$$

Where

$$D_x=\frac{E_x l^2 h}{2(1+\vartheta_x)} \quad \text{and} \quad D_y=\frac{E_y l^2 h}{2(1+\vartheta_y)}$$

are the additional flexural rigidities due to the microstructure. m_x and m_y are the coefficients of mutual influence which depends upon the elastic constants and fibre orientation. The relations for these coefficients can be written as [43]

$$\left.\begin{aligned} m_x &= \sin 2\beta\left\{\tfrac{\vartheta_x}{E_x}+\tfrac{1}{E_y}-\tfrac{1}{2G_{xy}}-(\cos^2\beta)\left(\tfrac{1}{E_x}+\tfrac{2\vartheta_x}{E_x}+\tfrac{1}{E_y}-\tfrac{1}{G_{xy}}\right)\right\} \\ m_y &= \sin 2\beta\left\{\tfrac{\vartheta_x}{E_x}+\tfrac{1}{E_y}-\tfrac{1}{2G_{xy}}-(\sin^2\beta)\left(\tfrac{1}{E_x}+\tfrac{2\vartheta_x}{E_x}+\tfrac{1}{E_y}-\tfrac{1}{G_{xy}}\right)\right\} \end{aligned}\right\}. \tag{2.3}$$

In the present work, the governing equation of a cracked orthotropic plate derived in [43] is further used to get the relation for critical buckling temperature and fundamental frequency. The assumptions involved in the formulation are taken according to classical plate theory for thin plates [11,45].

2.1 Relationship between the crack tip stresses and the far-field stresses

In the available literature, it is found that Rice and Levy [37] derived an approximate relation between tensile and bending stresses at the location of the crack and the nominal and bending stresses at the far sides of the plate. The line spring model given by Rice and Levy [37], reduces the purely three-dimensional problem into a two-dimensional problem. In [14–16], line spring model is used for the formulation of crack terms. King [29], developed a simplified line spring model considering that the part through the surface crack is the combination of a through crack and an edge crack. Joshi et al. [23] further modified these relations for a specially orthotropic plate. Extending their work Joshi et al. [24, 25] have also proposed the relations for crack terms in presence of thermal effects for the isotropic and orthotropic plates. Similar relations for in-plane forces n_y and bending moments m_y for the cracked orthotropic plate can be proposed as

$$m_y=-\frac{2a}{3\left(\frac{\alpha_{bt}}{6}+\alpha_{bb}\right)(3+\vartheta_x)(1-\vartheta_x)h+2a}M_{y^*}, \tag{2.4a}$$

$$n_y=\frac{2a}{(6\alpha_{bt}+\alpha_{tt})(1-\vartheta_x^2)h+2a}N_{Ty}. \tag{2.4b}$$

Where, α_{bb}, α_{tt} and $\alpha_{bt}=\alpha_{tb}$ are compliance coefficients used to match stretching and bending resistance of symmetric loading. The values for these coefficients can be found in [6]. For the arbitrary location of the crack along the x-axis, the above compliance coefficients are multiplied by

$$\left(2\Big/\sqrt{\pi\left(\frac{\gamma}{\Gamma}\right)}\right)\exp\left(-\left(\frac{(\Gamma-\xi_c)^2L_1^2}{\left(\frac{\gamma}{\Gamma}\right)}\right)\right),$$

here $\xi_c = d/L_1$ is the eccentricity ratio, d is the offset distance between the plate centre and centre of the crack, $\gamma=(h/L_1)$ and $\Gamma=(a/L_1)$. Similar formulation for considering of the effect of crack location can be found in the work of Gupta et al. [11], Joshi et al. [22], Gupta et al. [9] and Bose et al. [6]. Hence, the influence of change in crack location can be determined by using the appropriate compliance coefficients.

On substituting Eqs. (2.4a) and (2.4b) in Eq. (2.2) and expressing the moments M_y^* in form of lateral deflection (w) from [43], one can obtain the required governing equation of cracked orthotropic plate as

$$
\begin{aligned}
&\frac{\left(D_x+D^{lx}\right)\left\{\left(\frac{\partial^4 w}{\partial x^4}+\vartheta_y\frac{\partial^4 w}{\partial x^2\partial y^2}\right)+\frac{\left(\vartheta_y m_y+m_x\right)}{\frac{1}{G_{xy}}-m_y^2E_y}\left(2\frac{\partial^4 w}{\partial x^3\partial y}+m_yE_y\frac{\partial^4 w}{\partial x^2\partial y^2}\right)\right\}}{1-\frac{E_x\left(\vartheta_y m_y+m_x\right)}{\left(1-\vartheta_x\vartheta_y\right)\left(\frac{1}{G_{xy}}-m_y^2E_y\right)}\left(m_x+m_y\vartheta_x\frac{E_y}{E_x}\right)}\\
&+\frac{2\left\{\begin{array}{c}\frac{h^3}{6}\frac{\partial^4 w}{\partial x^2\partial y^2}+\left(\left(D_x+D^{lx}\right)m_x+\vartheta_x\left(D_y+D^{ly}\right)m_y\right)\frac{\partial^4 w}{\partial x^3\partial y}\\ +\left(\left(D_y+D^{ly}\right)m_y+\vartheta_y\left(D_x+D^{lx}\right)m_x\right)\frac{\partial^4 w}{\partial y^3\partial x}\end{array}\right\}}{\frac{1}{G_{xy}}-\frac{m_xE_x\left(\vartheta_y m_y+m_x\right)+m_yE_y\left(\vartheta_x m_x+m_y\right)}{\left(1-\vartheta_x\vartheta_y\right)}}\\
&+\frac{\left(D_y+D^{ly}\right)\left\{\left(\frac{\partial^4 w}{\partial y^4}+\vartheta_x\frac{\partial^4 w}{\partial x^2\partial y^2}\right)+\frac{\left(\vartheta_x m_x+m_y\right)}{\frac{1}{G_{xy}}-m_x^2E_x}\left(2\frac{\partial^4 w}{\partial y^3\partial x}+m_xE_x\frac{\partial^4 w}{\partial x^2\partial y^2}\right)\right\}}{1-\frac{E_y\left(\vartheta_x m_x+m_y\right)}{\left(1-\vartheta_x\vartheta_y\right)\left(\frac{1}{G_{xy}}-m_x^2E_x\right)}\left(m_y+m_x\vartheta_y\frac{E_x}{E_y}\right)}\\
&=-\rho h\frac{\partial^2 w}{\partial t^2}+\frac{2a}{3\left(\frac{\alpha_{bt}}{6}+\alpha_{bb}\right)(3+\vartheta_x)(1-\vartheta_x)h+2a}\\
&\times\left[\frac{\left(D_y+D^{ly}\right)\left\{\left(\frac{\partial^4 w}{\partial y^4}+\vartheta_x\frac{\partial^4 w}{\partial x^2\partial y^2}\right)+\frac{\left(\vartheta_x m_x+m_y\right)}{\frac{1}{G_{xy}}-m_x^2E_x}\left(2\frac{\partial^4 w}{\partial y^3\partial x}+m_xE_x\frac{\partial^4 w}{\partial x^2\partial y^2}\right)\right\}}{1-\frac{E_y\left(\vartheta_x m_x+m_y\right)}{\left(1-\vartheta_x\vartheta_y\right)\left(\frac{1}{G_{xy}}-m_x^2E_x\right)}\left(m_y+m_x\vartheta_y\frac{E_x}{E_y}\right)}+\frac{\partial^4 M_{Ty}}{\partial y^4}\right]-N_{Tx}\frac{\partial^2 w}{\partial x^2}\\
&-2N_{Txy}\frac{\partial^2 w}{\partial x\partial y}-\frac{(1+2a)}{(6\alpha_{bt}+\alpha_{tt})(1-v_x^2)h+2a}N_{Ty}\frac{\partial^2 w}{\partial y^2}-\frac{\partial^2 M_{Tx}}{\partial x^2}-\frac{\partial^2 M_{Ty}}{\partial y^2}+P_z. \qquad (2.5)
\end{aligned}
$$

3 Solution of governing equation

For the approximate solution of above differential governing equation (Eq. (2.3)), the Galerkin's method is used by defining the trail modal functions. These modal functions are chosen to satisfy all the kinematic boundary conditions. We can express the lateral displacement (w) of the plate in form of modal functions as [6]

$$w(x,y,t)=\sum_{n=1}^{\infty}\sum_{m=1}^{\infty}A_{mn}X_mY_n\phi_{mn}(t). \qquad (3.1)$$

In the above equation X_m and Y_n are the trail modal functions, A_{mn} is the arbitrary amplitude and $\phi_{mn}(t)$ is the time dependent function. The trail modal functions for the two

different boundary conditions (SSSS and CCSS) used in present study can be found in literature [15,24,26].

In the governing equation Eq. (2.2) of cracked orthotropic plate, the thermal effects are included in the form of thermal moments (M_{Tx}, M_{Ty} and M_{Txy}) and in-plane thermal forces (N_{Tx} , N_{Ty} and N_{Txy}). It is known that in different industrial applications, thin plate structures are used with a little temperature gradient and good thermal conductivity. Thus for simplification of present work, the solution for the above governing equation is given for the case of uniformly heated plates ($M_{Tx}=M_{Ty}=M_{Txy}=0$) with in-plane deflections restricted. It means the thermal moments are neglected and only the in-plane thermal forces (N_{Tx}, N_{Ty} and N_{Txy}) are considered. For uniformly heated plates, the constant in-plane thermal forces can be written in terms of lateral deflection as [43];

$$N_{Tx}=\frac{E_x T_c h}{\left(1-\vartheta_x\vartheta_y\right)}\left(\frac{\left(\vartheta_y m_y+m_x\right)\left(\alpha_{xy}+m_y E_y\alpha_y\right)}{\left(\frac{1}{G_{xy}}-m_y^2E_y\right)}+\left(\alpha_x+\alpha_y\vartheta_y\right)\right), \tag{3.2a}$$

$$N_{Ty}=\frac{E_y T_c h}{\left(1-\vartheta_x\vartheta_y\right)}\left(\frac{\left(\vartheta_x m_x+m_y\right)\left(\alpha_{xy}+m_x E_x\alpha_x\right)}{\left(\frac{1}{G_{xy}}-m_x^2E_x\right)}+\left(\alpha_x\vartheta_x+\alpha_y\right)\right), \tag{3.2b}$$

$$N_{Txy}=\frac{T_c h\left(\alpha_{xy}+m_x E_x\left(\alpha_x+\alpha_y\vartheta_y\right)+m_y E_y\left(\alpha_y+\alpha_x\vartheta_x\right)\right)}{\left(1-\vartheta_x\vartheta_y\right)}. \tag{3.2c}$$

Where, α_x, α_y and α_{xy} are the coefficients of thermal expansion. T_c is the rise in temperature above which the plate is stress-free.

On employing Eq. (3.1) and Eq. (3.2) in Eq. (2.5) and multiplying Eq. (2.5) by X_mY_n and then integrating over plate area, the governing equation of plate can be stated as;

$$\begin{aligned}
&\rho h\sum_{n=1}^{\infty}\sum_{m=1}^{\infty}A_{mn}\int_0^{L1}\int_0^{L2}X_m^2Y_n^2dxdy\frac{\partial^2\phi_{mn}(t)}{\partial t^2}\\
&+\sum_{n=1}^{\infty}\sum_{m=1}^{\infty}A_{mn}\phi_{mn}(t)\int_0^{L1}\int_0^{L2}\left\{\frac{\left(D_x+D^{lx}\right)\left\{\left(X_m^{iv}Y_n+\vartheta_yX_m^{ii}y_n^{ii}\right)+\frac{\left(\vartheta_y m_y+m_x\right)}{\frac{1}{G_{xy}}-m_y^2E_y}\left(2X_m^{iii}y_n^{i}+m_yE_yX_m^{ii}y_n^{ii}\right)\right\}}{1-\frac{E_x\left(\vartheta_y m_y+m_x\right)}{\left(1-\vartheta_x\vartheta_y\right)\left(\frac{1}{G_{xy}}-m_y^2E_y\right)}\left(m_x+m_y\vartheta_x\frac{E_y}{E_x}\right)}\right.\\
&+\frac{2\left\{\frac{h^3}{6}X_m^{ii}y_n^{ii}+\left(\left(D_x+D^{lx}\right)m_x+\vartheta_x\left(D_y+D^{ly}\right)m_y\right)X_m^{iii}y_n^{i}+\left(\left(D_y+D^{ly}\right)m_y+\vartheta_y\left(D_x+D^{lx}\right)m_x\right)X_m^{i}y_n^{iii}\right\}}{\frac{1}{G_{xy}}-\frac{m_xE_x\left(\vartheta_y m_y+m_x\right)+m_yE_y\left(\vartheta_x m_x+m_y\right)}{\left(1-\vartheta_x\vartheta_y\right)}}\\
&\left.+\frac{\left(D_y+D^{ly}\right)\left\{\left(Y_n^{iv}X_m+\vartheta_xX_m^{ii}y_n^{ii}\right)+\frac{\left(\vartheta_x m_x+m_y\right)}{\frac{1}{G_{xy}}-m_x^2E_x}\left(2X_m^{i}y_n^{iii}+m_xE_xX_m^{ii}y_n^{ii}\right)\right\}}{1-\frac{E_y\left(\vartheta_x m_x+m_y\right)}{\left(1-\vartheta_x\vartheta_y\right)\left(\frac{1}{G_{xy}}-m_x^2E_x\right)}\left(m_y+m_x\vartheta_y\frac{E_x}{E_y}\right)}\right\}
\end{aligned}$$

$$-\frac{2a}{3\left(\frac{\alpha_{bt}}{6}+\alpha_{bb}\right)(3+\vartheta_x)(1-\vartheta_x)h+2a}\frac{\left(D_y+D^{ly}\right)\left\{\left(Y_n^{iv}X_m+\vartheta_x X_m^{\text{ii}}y_n^{\text{ii}}\right)+\frac{\left(\vartheta_x m_x+m_y\right)}{\frac{1}{G_{xy}}-m_x^2E_x}\left(2X_m^i y_n^{iii}+m_xE_xX_m^{ii}y_n^{ii}\right)\right\}}{1-\frac{E_y\left(\vartheta_x m_x+m_y\right)}{\left(1-\vartheta_x\vartheta_y\right)\left(\frac{1}{G_{xy}}-m_x^2E_x\right)}\left(m_y+m_x\vartheta_y\frac{E_x}{E_y}\right)}$$

$$+\frac{E_xT_ch}{\left(1-\vartheta_x\vartheta_y\right)}\left(\frac{\left(\vartheta_y m_y+m_x\right)\left(\alpha_{xy}+m_yE_y\alpha_y\right)}{\left(\frac{1}{G_{xy}}-m_y^2E_y\right)}+\left(\alpha_x+\alpha_y\vartheta_y\right)\right)X_m^{ii}Y_n$$

$$+\left(1+\frac{2a}{\left(6\alpha_{bt}+\alpha_{tt}\right)\left(1-\vartheta_x^2\right)h+2a}\right)\frac{E_yT_ch}{\left(1-\vartheta_x\vartheta_y\right)}\left(\frac{\left(\vartheta_x m_x+m_y\right)\left(\alpha_{xy}+m_xE_x\alpha_x\right)}{\left(\frac{1}{G_{xy}}-m_x^2E_x\right)}+\left(\alpha_x\vartheta_x+\alpha_y\right)\right)Y_n^{ii}X_m$$

$$+2\left(\frac{T_ch\left(\alpha_{xy}+m_xE_x\left(\alpha_x+\alpha_y\vartheta_y\right)+m_yE_y\left(\alpha_y+\alpha_x\vartheta_x\right)\right)}{\left(1-\vartheta_x\vartheta_y\right)}\right)X_m^iy_n^i\Bigg\}X_mY_ndxdy$$

$$=\int_0^{l_2}\int_0^{l_2}P_zX_mY_ndxdy. \tag{3.3}$$

Based on the application of the appropriate delta function, the lateral load P_z can be readily expressed as [15]

$$P_z=P_0(t)\delta(x-x_0)\delta(y-y_0).$$

Where, $P_0(t)$ denotes the time-dependent lateral load and (x_0,y_0) is the position coordinate of the load.

On substituting P_z from Eq. (3.2) into Eq. (3.1), the force term of Eq. (3.1) can be expressed as

$$\begin{aligned}P_{mn}&=P_0(t)\int_0^{l_1}\int_0^{l_2}\delta(x-x_0)\delta(y-y_0)X_mY_ndxdy,\\P_{mn}&=P_0(t)X_m(x_0)Y_n(y_0),\\P_{mn}&=P_0(t)Q_{mn}.\end{aligned}$$

Where, $Q_{mn}=X_m(x_0)Y_n(y_0)$ shows the position of lateral load $(P_0(t))$ on plate for different boundary conditions.

The lateral load p_z can be neglected for free vibrations. On expressing Eq. (3.3) in the form of Duffing equation as

$$M_{mn}\frac{\partial^2\phi_{mn}(t)}{\partial t^2}+K_{mn}\phi_{mn}(t)=0, \tag{3.4}$$

where

$$M_{mn}=\rho h\sum_{n=1}^{\infty}\sum_{m=1}^{\infty}A_{mn}\int_0^{L1}\int_0^{L2}{X_m}^2{Y_n}^2dxdy, \tag{3.5a}$$

$$K_{mn}=\sum_{n=1}^{\infty}\sum_{m=1}^{\infty}A_{mn}\phi_{mn}(t)\int_0^{L1}\int_0^{L2}\left\{\frac{\left(D_x+D^{Lx}\right)\left\{\left(X_m^{iv}Y_n+\vartheta_yX_m^{ii}y_n^{ii}\right)+\frac{\left(\vartheta_ym_y+m_x\right)}{\frac{1}{G_{xy}}-m_y^2E_y}\left(2X_m^{iii}y_n^i+m_yE_yX_m^{ii}y_n^{ii}\right)\right\}}{1-\frac{E_x\left(\vartheta_ym_y+m_x\right)}{\left(1-\vartheta_x\vartheta_y\right)\left(\frac{1}{G_{xy}}-m_y^2E_y\right)}\left(m_x+m_y\vartheta_x\frac{E_y}{E_x}\right)}\right.$$

$$+\frac{2\left\{\frac{h^3}{6}X_m^{ii}y_n^{ii}+\left(\left(D_x+D^{lx}\right)m_x+\vartheta_x\left(D_y+D^{ly}\right)m_y\right)X_m^{iii}y_n^{i}+\left(\left(D_y+D^{ly}\right)m_y+\vartheta_y\left(D_x+D^{lx}\right)m_x\right)X_m^{i}y_n^{iii}\right\}}{\frac{1}{G_{xy}}-\frac{m_xE_x\left(\vartheta_ym_y+m_x\right)+m_yE_y\left(\vartheta_xm_x+m_y\right)}{\left(1-\vartheta_x\vartheta_y\right)}}$$

$$+\frac{\left(D_y+D^{ly_y}\right)\left\{\left(Y_n^{iv}X_m+\vartheta_xX_m^{ii}y_n^{ii}\right)+\frac{\left(\vartheta_xm_x+m_y\right)}{\frac{1}{G_{xy}}-m_x^2E_x}\left(2X_m^{i}y_n^{iii}+m_xE_xX_m^{ii}y_n^{ii}\right)\right\}}{1-\frac{E_y\left(\vartheta_xm_x+m_y\right)}{\left(1-\vartheta_x\vartheta_y\right)\left(\frac{1}{G_{xy}}-m_x^2E_x\right)}\left(m_y+m_x\vartheta_y\frac{E_x}{E_y}\right)}$$

$$-\frac{2a}{3\left(\frac{\alpha_{bt}}{6}+\alpha_{bb}\right)(3+\vartheta_x)(1-\vartheta_x)h+2a}\frac{\left(D_y+D^{ly}\right)\left\{\left(Y_n^{iv}X_m+\vartheta_xX_m^{ii}y_n^{ii}\right)+\frac{\left(\vartheta_xm_x+m_y\right)}{\frac{1}{G_{xy}}-m_x^2E_x}\left(2X_m^{i}y_n^{iii}+m_xE_xX_m^{ii}y_n^{\mathrm{ii}}\right)\right\}}{1-\frac{E_y\left(\vartheta_xm_x+m_y\right)}{\left(1-\vartheta_x\vartheta_y\right)\left(\frac{1}{G_{xy}}-m_x^2E_x\right)}\left(m_y+m_x\vartheta_y\frac{E_x}{E_y}\right)}$$

$$+\frac{E_xT_ch}{\left(1-\vartheta_x\vartheta_y\right)}\left(\frac{\left(\vartheta_ym_y+m_x\right)\left(\alpha_{xy}+m_yE_y\alpha_y\right)}{\left(\frac{1}{G_{xy}}-m_y^2E_y\right)}+\left(\alpha_x+\alpha_y\vartheta_y\right)\right)X_m^{\mathrm{iu}}Y_n$$

$$+\left(1+\frac{2a}{(6\alpha_{bt}+\alpha_{tt})\left(1-\vartheta_x^{22}h+2a\right.}\right)\frac{E_yT_ch}{\left(1-\vartheta_x\vartheta_y\right)}\left(\frac{\left(\vartheta_xm_x+m_y\right)\left(\alpha_{xy}+m_xE_x\alpha_x\right)}{\left(\frac{1}{G_{xy}}-m_x^2E_x\right)}+\left(\alpha_x\vartheta_x+\alpha_y\right)\right)Y_n^{ii}X_m$$

$$+2\left(\frac{T_ch\left(\alpha_{xy}+m_xE_x\left(\alpha_x+\alpha_y\vartheta_y\right)+m_yE_y\left(\alpha_y+\alpha_x\vartheta_x\right)\right)}{\left(1-\vartheta_x\vartheta_y\right)}\right)X_m^{i}y_n^{j}\Bigg\}X_mY_ndxdy. \tag{3.5b}$$

From Eq. (3.5b), the fundamental frequency can be determined as $\omega_{mn}^2=K_{mn}/M_{mn}$.

4 Relationship for critical buckling temperature

In this section a classical relation for critical buckling temperature of a cracked orthotropic plate is presented using the equilibrium equation of plate. It is well known that the thermal buckling depends on the in-plane compressive forces induced by temperature rise. The relation of critical buckling temperature of an intact and cracked isotropic plate can be obtained in literature [5, 21, 45]. In present work the relationship for buckling temperature is derived by finding the equilibrium position between the stiffness and the thermal stresses of the plate from Eq. (3.3). For geometrically linear i.e., $M_{Tx}=M_{Ty}=M_{Txy}=0$ and constant in-plane compressive forces (Eq. (3.2)) due to uniform temperature rise N_{Tx}, N_{Ty} and N_{Txy}; only the static boundary conditions are to be satisfied. So, in the absence of thermal bending moment and the presence of constant in-plane thermal forces the equation of equilibrium for buckling phenomenon of cracked orthotropic micro plate can be written as

$$\frac{-\left(D_x+D^{lx}\right)\left\{\left(\frac{\partial^4w}{\partial x^4}+\vartheta_y\frac{\partial^4w}{\partial x^2\partial y^2}\right)+\frac{\left(\vartheta_ym_y+m_x\right)}{\frac{1}{G_{xy}}-m_y^2E_y}\left(2\frac{\partial^4w}{\partial x^3\partial y}+m_yE_y\frac{\partial^4w}{\partial x^2\partial y^2}\right)\right\}}{1-\frac{E_x\left(\vartheta_ym_y+m_x\right)}{\left(1-\vartheta_x\vartheta_y\right)\left(\frac{1}{G_{xy}}-m_y^2E_y\right)}\left(m_x+m_y\vartheta_x\frac{E_y}{E_x}\right)}$$

$$+\frac{-2\left\{\frac{h^3}{6}\frac{\partial^4w}{\partial x^2\partial y^2}+\left(\left(D_x+D^{lx}\right)m_x+\vartheta_x\left(D_y+D^{ly}\right)m_y\right)\frac{\partial^4w}{\partial x^3\partial y}+\left(\left(D_y+D^{ly}\right)m_y+\vartheta_y\left(D_x+D^{lx}\right)m_x\right)\frac{\partial^4w}{\partial y^3\partial x}\right\}}{\frac{1}{G_{xy}}-\frac{m_xE_x\left(\vartheta_ym_y+m_x\right)+m_yE_y\left(\vartheta_xm_x+m_y\right)}{\left(1-\vartheta_x\vartheta_y\right)}}$$

$$
\begin{aligned}
&+\frac{-\left(D_y+D^{ly}\right)\left\{\left(\frac{\partial^4 w}{\partial y^4}+\vartheta_x\frac{\partial^4 w}{\partial x^2\partial y^2}\right)+\frac{\left(\vartheta_x m_x+m_y\right)}{\frac{1}{G_{xy}}-m_x^2E_x}\left(2\frac{\partial^4 w}{\partial y^3\partial x}+m_xE_x\frac{\partial^4 w}{\partial x^2\partial y^2}\right)\right\}}{1-\frac{E_y\left(\vartheta_x m_x+m_y\right)}{\left(1-\vartheta_x\vartheta_y\right)\left(\frac{1}{G_{xy}}-m_x^2E_x\right)}\left(m_y+m_x\vartheta_y\frac{E_x}{E_y}\right)}\\
&-\frac{2a}{3\left(\frac{\alpha_{bt}}{6}+\alpha_{bb}\right)(3+\vartheta_x)(1-\vartheta_x)h+2a}\frac{\left(D_y+D^{ly}\right)\left\{\left(\frac{\partial^4 w}{\partial y^4}+\vartheta_x\frac{\partial^4 w}{\partial x^2\partial y^2}\right)+\frac{\left(\vartheta_x m_x+m_y\right)}{\frac{1}{G_{xy}}-m_x^2E_x}\left(2\frac{\partial^3 w}{\partial y^2\partial x}+m_xE_x\frac{\partial^4 w}{\partial x^2\partial y^2}\right)\right\}}{1-\frac{E_y\left(\vartheta_x m_x+m_y\right)}{\left(1-\vartheta_x\vartheta_y\right)\left(\frac{1}{G_{xy}}-m_x^2E_x\right)}\left(m_y+m_x\vartheta_y\frac{E_x}{E_y}\right)}\\
=&-\frac{E_xT_ch}{\left(1-\vartheta_x\vartheta_y\right)}\left(\frac{\left(\vartheta_y m_y+m_x\right)\left(\alpha_{xy}+m_yE_y\alpha_y\right)}{\left(\frac{1}{G_{xy}}-m_y^2E_y\right)}+\left(\alpha_x+\alpha_y\vartheta_y\right)\right)\frac{\partial^2 w}{\partial x^2}\\
&-\frac{E_yT_ch}{\left(1-\vartheta_x\vartheta_y\right)}\left(1+\frac{2a}{\left(6\alpha_{bt}+\alpha_{tt}\right)\left(1-\vartheta_x^2\right)h+2a}\right)\left(\frac{\left(\vartheta_x m_x+m_y\right)\left(\alpha_{xy}+m_xE_x\alpha_x\right)}{\left(\frac{1}{G_{xy}}-m_x^2E_x\right)}+\left(\alpha_x\vartheta_x+\alpha_y\right)\right)\frac{\partial^2 w}{\partial y^2}\\
&-2\left(\frac{T_ch\left(\alpha_{xy}+m_xE_x\left(\alpha_x+\alpha_y\vartheta_y\right)+m_yE_y\left(\alpha_y+\alpha_x\vartheta_x\right)\right)}{\left(1-\vartheta_x\vartheta_y\right)}\right)\frac{\partial^2 w}{\partial x\partial y}.
\end{aligned}
\tag{4.1}
$$

From Eq. (4.1) the relationship for buckling temperature can be expressed as

$$
\begin{aligned}
&\frac{-\left(D_x+D^{ix}\right)\left\{\left(-\frac{m}{\partial x^4}+\vartheta_y\frac{\partial^4 w}{\partial x^2\partial y^2}\right)+\frac{\left(\vartheta_y m_y+m_x\right)}{\frac{1}{G_{xy}}-m_y^2E_y}\left(2\frac{\partial^4 w}{\partial x^3\partial y}+m_yE_y\frac{\partial^4 w}{\partial x^2\partial y^2}\right)\right\}}{1-\frac{E_x\left(\vartheta_y m_y+m_x\right)}{\left(1-\vartheta_x\vartheta_y\right)\left(\frac{1}{G_{xy}}-m_y^2E_y\right)}\left(m_x+m_y\vartheta_x\frac{E_y}{E_x}\right)}\\
&+\frac{-2\left\{\frac{h^3}{6}\frac{\partial^4 w}{\partial x^2\partial y^2}+\left(\left(D_x+D^{lx}\right)m_x+\vartheta_x\left(D_y+D^{ly}\right)m_y\right)\frac{\partial^4 w}{\partial x^3\partial y}+\left(\left(D_y+D^{(y}\right)m_y+\vartheta_y\left(D_x+D^{lx}\right)m_x\right)\frac{\partial^4 w}{\partial y^3\partial x}\right\}}{\frac{1}{G_{xy}}-\frac{m_xE_x\left(\vartheta_y m_y+m_x\right)+m_yE_y\left(\vartheta_x m_x+m_y\right)}{\left(1-\vartheta_x\vartheta_y\right)}}\\
&+\frac{-\left(D_y+D^{ly}\right)\left\{\left(\frac{\partial^4 w}{\partial y^4}+\vartheta_x\frac{\partial^4 w}{\partial x^2\partial y^2}\right)+\frac{\left(\vartheta_x m_x+m_y\right)}{\frac{1}{G_{xy}}-m_x^2E_x}\left(2\frac{\partial^4 w}{\partial y^3\partial x}+m_xE_x\frac{\partial^4 w}{\partial x^2\partial y^2}\right)\right\}}{1-\frac{E_y\left(\vartheta_x m_x+m_y\right)}{\left(1-\vartheta_x\vartheta_y\right)\left(\frac{1}{G_{xy}}-m_x^2E_x\right)}\left(m_y+m_x\vartheta_y\frac{E_x}{E_y}\right)}T\\
&-\frac{2a}{3\left(\frac{\alpha_{bt}}{6}+\alpha_{bb}\right)(3+\vartheta_x)(1-\vartheta_x)h+2a}\frac{\left(D_y+D^{ly}\right)\left\{\left(\frac{\partial^4 w}{\partial y^4}+\vartheta_x\frac{\partial^4 w}{\partial x^2\partial y^2}\right)+\frac{\left(\vartheta_x m_x+m_y\right)}{\frac{1}{G_{xy}}-m_x^2E_x}\left(2\frac{\partial^3 w}{\partial y^2\partial x}+m_xE_x\frac{\partial^4 w}{\partial x^2\partial y^2}\right)\right\}}{1-\frac{E_y\left(\vartheta_x m_x+m_y\right)}{\left(1-\vartheta_x\vartheta_y\right)\left(\frac{1}{G_{xy}}-m_x^2E_x\right)}\left(m_y+m_x\vartheta_y\frac{E_x}{E_y}\right)}\\
=&\frac{-\frac{E_xh}{\left(1-\vartheta_x\vartheta_y\right)}\left(\frac{\left(\vartheta_y m_y+m_x\right)\left(\alpha_{xy}+m_yE_y\alpha_y\right)}{\left(\frac{1}{G_{xy}}-m_y^2E_y\right)}+\left(\alpha_x+\alpha_y\vartheta_y\right)\right)\frac{\partial^2 w}{\partial x^2}}{}\\
&-\frac{E_yh}{\left(1-\vartheta_x\vartheta_y\right)}\left(1+\frac{2a}{\left(6\alpha_{bt}+\alpha_{tt}\right)\left(1-\vartheta_x^2\right)h+2a}\right)\left(\frac{\left(\vartheta_x m_x+m_y\right)\left(\alpha_{xy}+m_xE_x\alpha_x\right)}{\left(\frac{1}{G_{xy}}-m_x^2E_x\right)}+\left(\alpha_x\vartheta_x+\alpha_y\right)\right)\frac{\partial^2 w}{\partial y^2}\\
&-2\left(\frac{h\left(\alpha_{xy}+m_xE_x\left(\alpha_x+\alpha_y\vartheta_y\right)+m_yE_y\left(\alpha_y+\alpha_x\vartheta_x\right)\right)}{\left(1-\vartheta_x\vartheta_y\right)}\right)\frac{\partial^2 w}{\partial x\partial y}.
\end{aligned}
\tag{4.2}
$$

This relationship for buckling temperature depends upon the boundary conditions, for e.g., the solution for a simply supported (SSSS) and two adjacent edges are clamped while

the other two edges are simply supported (CCSS) boundary conditions can be written as

$$\text{For SSSS} \qquad w(x,y) = A_{mn}\sin(\alpha_m x)\sin(\beta_n y), \tag{4.3a}$$

$$\text{For CCSS} \qquad w(x,y) = A_{mn}\sin(\alpha_m x)\sin\left(\frac{\alpha_m x}{2}\right)\sin(\beta_n y)\sin\left(\frac{\beta_n y}{2}\right). \tag{4.3b}$$

Where

$$\alpha_m = \frac{m\pi}{L_1} \quad \text{and} \quad \beta_n = \frac{n\pi}{L_2}.$$

On substituting the solution of lateral deflection (w) from Eq. (4.3a) into Eq. (4.2) and placing the mode number $m = n = 1$, we can get the critical buckling temperature T_{bcr} from Eq. (4.2). Here T_{bcr} is calculated for $m = n = 1$ as for other values of m and n, the buckling temperature obtained is higher.

5 Results and discussion

In this section, the results for buckling temperature and its effect on fundamental frequency is presented for cracked orthotropic micro plate as a function of fibre orientation (β), uniform temperature rise (T^*), crack length (a/l_1), crack location (ξ_c), and length scale parameter (l/l_1). The above results are presented for two different SSSS and CCSS boundary condition. The rise in temperature is expressed in non-dimensional form as $T^* = T/T_{bcr}$, where T is the rise in temperature of orthotropic plate. Boron Epoxy is taken as plate material with following properties, $E_y = 18.9$GPa, $E_x = 208$GPa, $\vartheta_2 = 0.0208$, $\vartheta_1 = 0.23$, $G_{12} = 5.7$GPa, $\rho = 2000$kg/m^3. The crack depth to plate thickness ratio is taken constant as 0.6 throughout this work and the plate in-plane dimensions are $L_1 = L_2 = 1$m. The results for fundamental frequency as a function of critical buckling temperature for cracked orthotropic plate with fibre orientation in thermal domain are not available in literature, however the results are available for cracked isotropic plate in thermal domain. The present model can be easily reduced to the isotropic one by considering suitable material parameter for isotropic plate. Hence the present model holds good agreement with the existing results of [26] for isotropic plate as seen in Table 1.

Table 2 shows a comparison of results for the frequency parameter of an orthotropic plate as a function of fibre orientation, crack length and length scale parameter. The properties of the orthotropic plate for the validation in Table 2 are taken from [11]. It is observed from Table 2 that, there is an exact agreement between present results and the published results which verify the correctness of the present model when the effect of temperature is neglected.

Fig. 2(a) and Fig. 2(b) shows the variation of critical buckling temperature with crack length and fibre orientation for a cracked orthotropic SSSS and CCSS square plate $(l/l_1 = 0)$. It is observed that as the fibre orientation increases from 0° to 45°, the critical buckling temperature also rises and reaches a maximum value at 45°, this variation in critical

Table 1: Comparison of frequency $(\omega_{mn} l_1^2 \sqrt{\rho h/D})$ for intact and cracked isotropic CCSS $(m=n=1,\ l_1/l_2=1)$.

Temperature T^*	Intact plate		Cracked plate	
	Half crack length, $a/l_1=0.0$		Half crack length, $a/l_1=0.01$	
	present	[26]	present	[26]
0	28.35	28.35	27.50	27.50
0.1	26.89	26.89	26.00	26.00
0.2	25.35	25.35	24.51	24.51
0.3	23.72	23.72	22.93	22.93
0.4	21.96	21.96	21.23	21.23
0.5	20.05	20.05	19.38	19.38

Table 2: Comparison of frequency parameter for an orthotropic plate as a function of fibre orientation, crack length and length scale parameter. $L_1/L_2=1,\ \Delta T=0$.

Frequency parameter $(\rho h \omega_m n^2 L_1^4/\sqrt{D_x D_y})$					
Half crack length (a)	Fibre angle (β)	Length Scale parameter (l)			
		$l/l_1=0$ (CPT)		$l/l_1=0.001$ (MCST)	
		Present	[11]	Present	[11]
$a/l_1=0$	0	20.03	20.03	20.48	20.48
(Intact)	15	21.85	21.85	22.16	22.16
	30	25.08	25.08	25.31	25.31
	45	26.55	26.55	26.75	26.75
	60	25.08	25.08	25.31	25.31
	75	21.85	21.85	22.16	22.16
	90	20.03	20.03	20.48	20.48
$a/l_1=0.001$	0	19.89	19.89	20.33	20.33
(Cracked)	15	21.61	21.61	21.91	21.91
	30	24.84	24.84	25.05	25.05
	45	26.32	26.32	26.51	26.51
	60	24.83	24.83	25.05	25.05
	75	21.41	21.41	21.71	21.71
	90	18.86	18.86	19.27	19.27

buckling temperature from 0° to 45° fibre orientation is worth noting as the critical buckling temperature at 45° is almost five times the critical buckling temperature at 0°. The result in Fig. 2 also shows the effect of crack length on the critical buckling temperature with fibre orientation. It is observed that as the crack length increases the critical buckling temperature decreases when compared to their intact counterpart. One more interesting point to note in Fig. 2 is that the critical buckling temperature for cracked plate is not symmetric about 45° like the one seen for an intact plate. This is because the crack is kept constant along the x-axis while the fibre orients from 0° to 45°, hence the stiffness of the plate is least affected when the crack is parallel to the fibre (0°) and most affected when the crack is across the fibre (90°). Fig. 2(c) and Fig. 2(d) shows a similar result for micro-sized orthotropic plate $(l/l_1=0.001)$. The results are higher when compared to Fig. 2(a) and Fig. 2(b) due to the consideration of additional bending rigidity arising due to consideration of internal material length scale parameter based on modified couple stress theory.

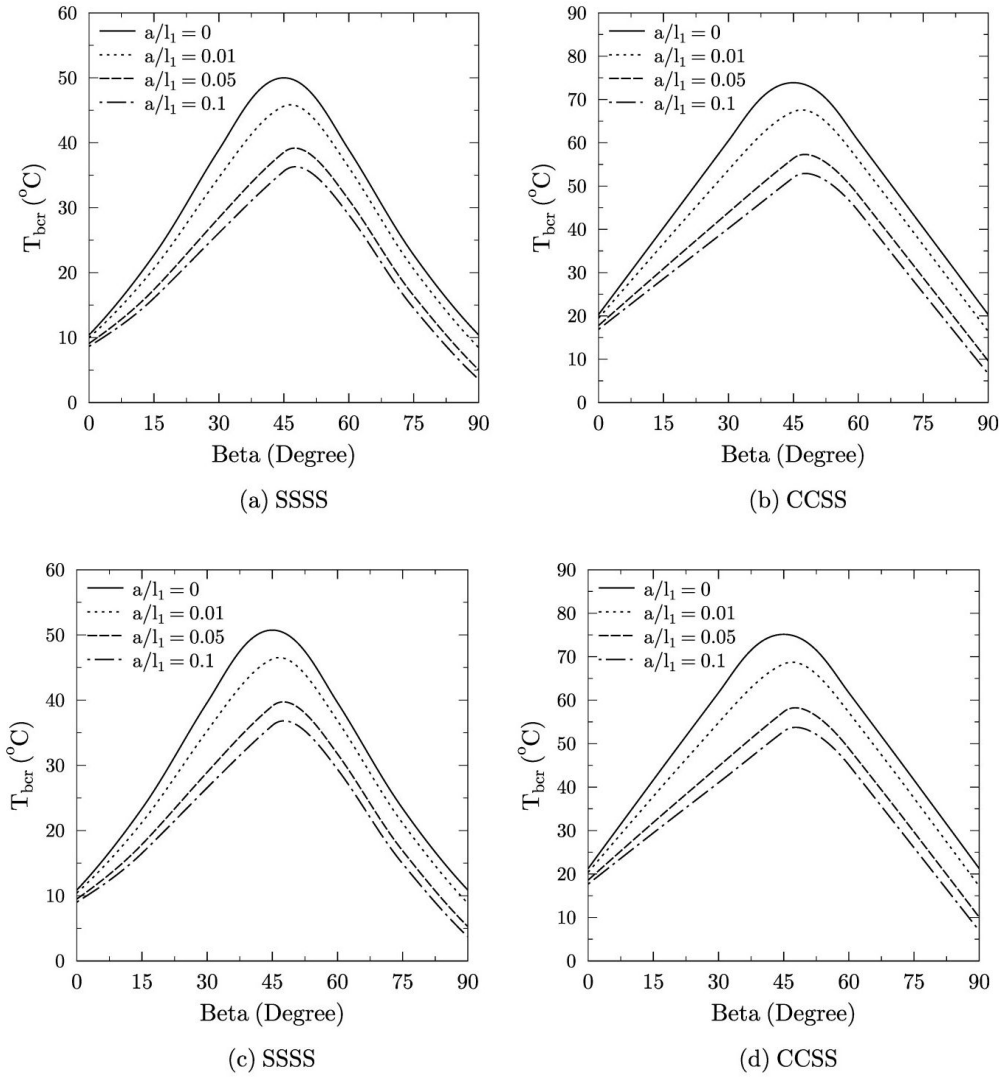

Figure 2: Critical buckling temperature (°) as affected by crack length for various fibre orientations. (a) and (b) -CPT $(l/l_1=0)$ and (c) and (d) -MCST $(l/l_1=0.001)$.

The variation in critical buckling temperature (T_{bcr}) of cracked orthotropic micro-plate as with various material length scale parameter and fibre orientation is shown in Fig. 3 for SSSS and CCSS boundary conditions. It is found that for fixed orientation of fibres, the buckling temperature increases with the increase in length scale parameter. Although the change in buckling temperature is quantitatively different for SSSS and CCSS boundary conditions, the effect of crack length, fibre orientation and material length scale parame-

Table 3: Critical buckling temperature $(^\circ C)$ for micro plate as affected by crack location for various fibre orientations $(a/l_1=0.2,\ l/l_1=0.001)$.

Critical Buckling Temperature (T_{bcr})				
Boundary conditions	β	Crack location		
		$\xi_c=0$	$\xi_c=0.1$	$\xi_c=0.2$
SSSS	0	9.104	9.520	9.660
	15	16.739	17.946	18.391
	30	26.932	29.065	29.870
	45	36.600	39.243	40.209
	60	29.795	31.868	32.596
	75	15.237	16.981	17.590
	90	3.963	5.337	5.832
CCSS	0	17.835	18.642	18.913
	15	29.837	31.985	32.777
	30	41.601	44.963	46.233
	45	53.541	57.548	59.016
	60	45.726	49.073	50.252
	75	26.652	29.854	30.975
	90	7.461	10.202	11.189

ter for CCSS plate is principally same for both SSSS and CCSS plate.

Table 3 shows the critical buckling temperature of cracked micro-plate as affected by crack location and fibre orientation. It has been observed that for a fixed crack length $a/l_1=0.2$ and length scale parameter $l/l_1=0.001$, as the crack moves away from the centre the critical buckling temperature increases for all orientations of fibres, this is because at the centre of the plate, the crack affects plate's stiffness to the maximum. From Table 3, it is also seen that the reduction in stiffness is more pronounced fibre orientation 90° than for 0°.

Fig. 4 shows the variation of frequency as affected by temperature rise (T^*) and fibre orientation (β) for SSSS and CCSS boundary conditions. It is seen that as the temperature rises the fundamental frequency decreases, it is due to the reduction in thermal stiffness of the plate. It is also observed that as the fibre orientation increases from 0° to 45°, the frequency also rises till 45° and a symmetrical pattern is obtained thereafter for an intact orthotropic plate (Figs. 4(a) and (b)). However, for a cracked plate (Figs. 4(c) and (d)) the frequency variation is not symmetric about 45° as the fibres are differently affected by a crack at each fibre orientation. Hence, the present result brings out an important conclusion that the frequency can be altered with the help of fibre orientation for an orthotropic plate under thermal environment. Also, the effect of crack on stiffness of the plate can be minimized by selecting optimum fibre orientation.

The variation in the fundamental frequency with length scale parameter and fibre orientation for a cracked orthotropic micro-plate is presented in Fig. 5. It is seen that for both SSSS and CCSS plate, the pattern of frequency variation with fibre orientation

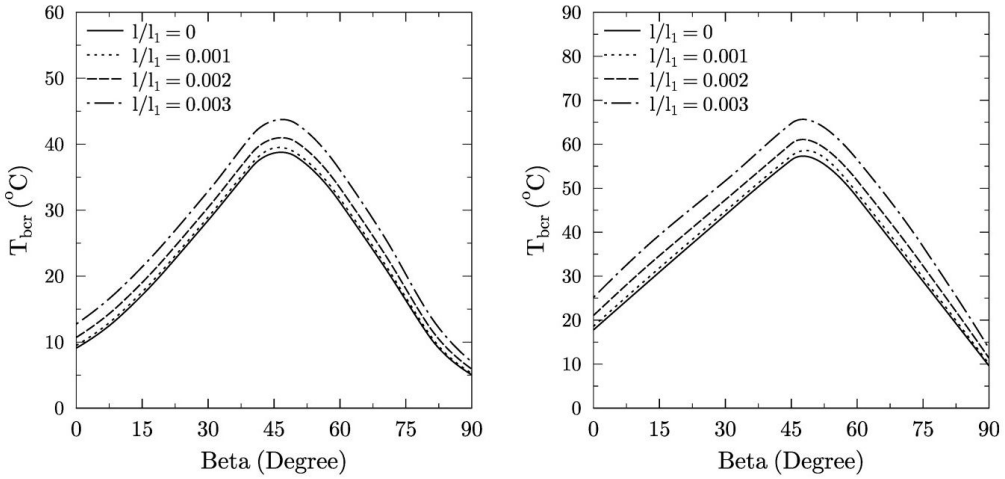

Figure 3: Critical buckling temperature (°) for cracked orthotropic plate as affected by internal material length scale parameter for various fibre orientations $(a/l_1=0.05)$.

is the same as in Fig. 4. On comparing the results for frequency obtained using CPT $(l/l_1=0)$ and MCST $(l/l_1\neq 0)$ in Fig. 5, it is found that for a given value of $a/l_1=0.05$ and $T^*=0.1$ the frequency increases with increase in length scale parameter. This increase in frequency is due to increased flexural rigidity which adds to the stiffness of plate. A similar change in frequency is also observed in [11] for intact and cracked orthotropic plate in the absence of thermal effects. In the present work, such variation is also found to be true in the case of cracked orthotropic plate in thermal domain (Fig. 5). Thus, the application of length scale parameter to consider the effect of microstructure is significant in thermal domain as well.

Effect of crack location on frequency of cracked orthotropic micro-plate as affected by non-dimensional temperature T^* is shown in Table 4 and Table 5 for SSSS and CCSS boundary conditions respectively. For a fixed length scale parameter $l/l_1=0.001$, length of crack $a/l_1=0.2$ and fibre orientation $\beta=45°$, it is observed that as the crack moves away from the centre from $\xi_c=0$ to 0.2; the fundamental frequency increases. It means frequency is more affected when crack is located at the centre and least affected when it moves away from centre.

Fig. 6 shows an important comparison between results obtained by CPT and MCST for critical buckling temperature as affected by the plate dimensions. In order to change the plate dimensions uniformly, plate length to plate thickness ratio is kept constant at $L_1/h=100$ and $L_1=L_2$. It can be seen in Fig. 6 that as the plate dimension reduces the CPT starts under-predicting the critical buckling temperature thereby reflecting the contribution of internal material length scale parameter on flexural rigidity of micro-sized

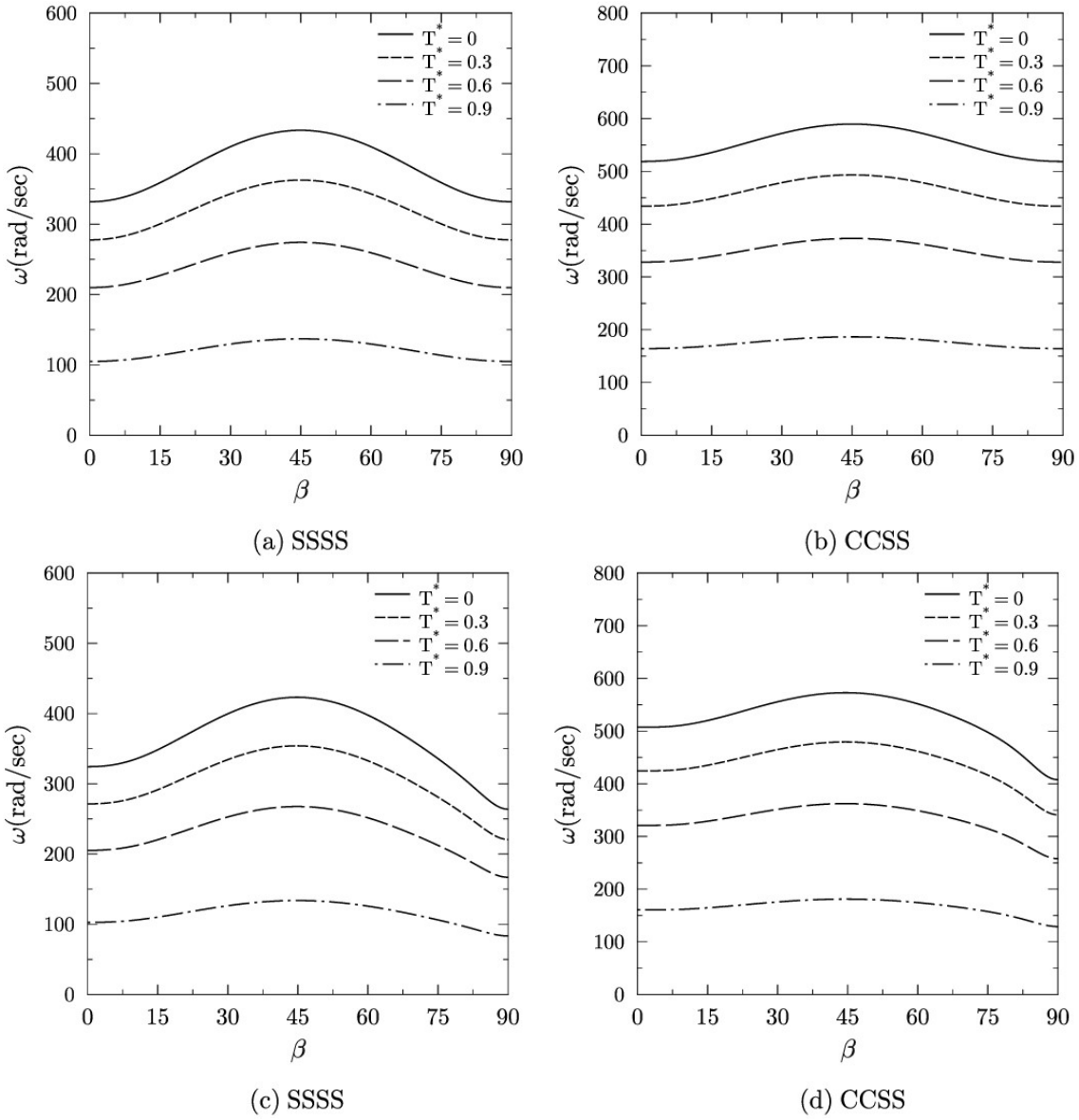

Figure 4: Fundamental frequency of an orthotropic plate as a function of temperature (T^*) and fibre orientation (β) for $l/l_1 = 0.001$. (a) and (b) -Intact. (c) and (d) -Cracked $(a/l_1 = 0.05)$.

plates. The differences in result between both the theories are found in the case of intact as well as cracked plate and for both SSSS and CCSS boundary conditions.

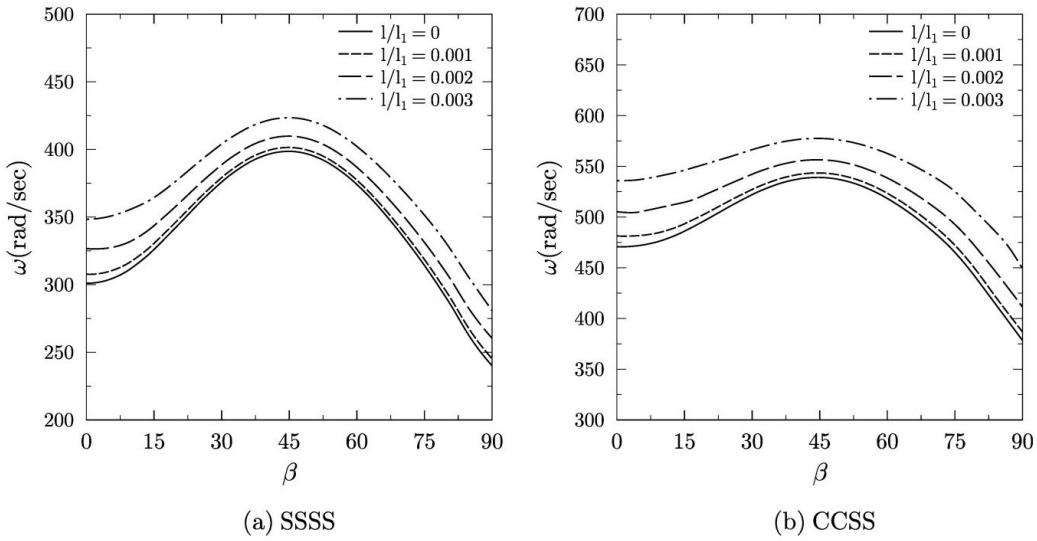

Figure 5: Fundamental frequency of an orthotropic plate as a function of length scale parameter (l) and fibre orientation (β) for $T^* = 0.1$ and $a/l_1 = 0.05$.

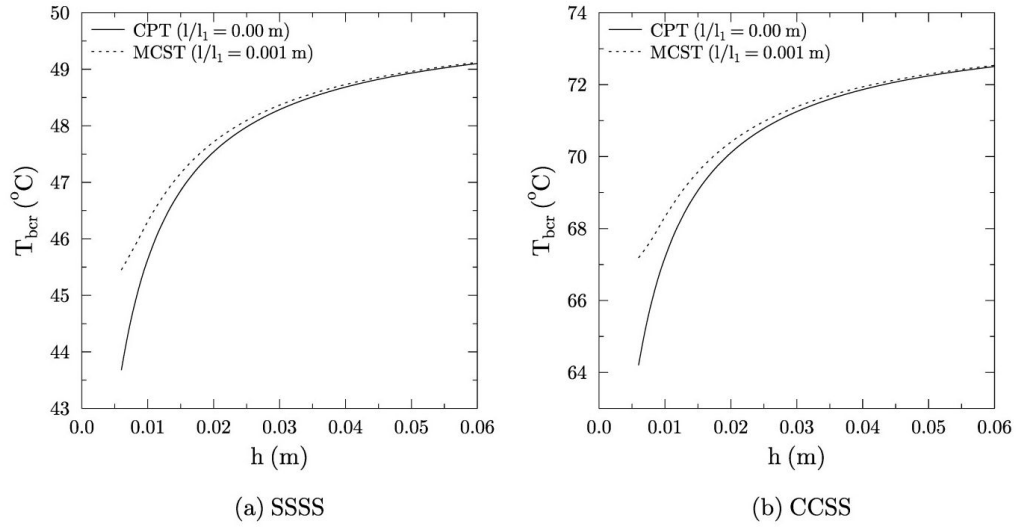

Figure 6: Variation of critical buckling temperature with plate size $(L_1/h = 100)$, $(L_1 = L_2)$.

6 Conclusions

The obtained results are helpful in designing the structures comprising of orthotropic plates which are subjected to a thermal environment. As per the author's knowledge, this

Table 4: Fundamental frequency for a cracked orthotropic SSSS micro plate $(a/l_1=0.2)$ as affected by crack location $(l/l_1=0.001,\ \beta=45^\circ)$.

T^*	Fundamental Frequency (rad/s)		
	$\xi_c=0$	$\xi_c=0.1$	$\xi_c=0.2$
0	420.856	423.283	424.160
0.1	399.259	401.561	402.394
0.2	376.425	378.596	379.380
0.3	352.113	354.144	354.878
0.4	325.994	327.873	328.553
0.5	297.590	299.306	299.926
0.6	266.173	267.707	268.262
0.7	230.512	231.841	232.322
0.8	188.213	189.298	189.690
0.9	133.086	133.854	134.131

Table 5: Fundamental frequency for a cracked orthotropic CCSS micro plate $(a/l_1=0.2)$ as affected by crack location $(l/l_1=0.001,\ \beta=45^\circ)$.

T^*	Fundamental Frequency (rad/s)		
	$\xi_c=0$	$\xi_c=0.1$	$\xi_c=0.2$
0	569.102	573.085	574.523
0.1	539.897	543.676	545.041
0.2	509.020	512.582	513.869
0.3	476.145	479.477	480.681
0.4	440.824	443.909	445.024
0.5	402.416	405.232	406.249
0.6	359.931	362.450	363.360
0.7	311.710	313.891	314.679
0.8	254.510	256.291	256.934
0.9	179.966	181.225	181.680

is the first attempt to analytically quantify the critical buckling temperature as affected by fibre orientation, size effects and effect of crack.

The present analytical model is also capable to capture the size-effect and hence can be applied in optimum designing of orthotropic micro-plates. Micro-plates are frequently used as sensing devices and are often subjected to different surroundings like fluidic medium and thermal environment.

Results are presented for critical buckling temperature and its effect on fundamental frequency for various parameters like crack length, fibre orientation and length scale parameter. It is concluded that by varying the fibre orientation, the critical buckling temperature can be altered to a large extent. Further, the present work explains the importance of the length scale parameter for a micro-sized plate and concludes that the length scale parameter has a positive impact on critical buckling temperature. The importance of size-effect on critical buckling temperatures is shown by comparing the result obtained

using CPT and MCST.

References

[1] B. AKGÖZ AND Ö. CIVALEK, *Free vibration analysis of axially functionally graded tapered Bernoulli-Euler microbeams based on the modified couple stress theory,* Compos. Struct., 98 (2013), pp. 314–322.

[2] B. AKGÖZ AND Ö. CIVALEK, *Modeling and analysis of micro-sized plates resting on elastic medium using the modified couple stress theory,* Meccanica, 48 (2013), pp. 863–873.

[3] B. AKGÖZ AND Ö. CIVALEK, *A microstructure-dependent sinusoidal plate model based on the strain gradient elasticity theory,* Acta Mech., 226 (2015), pp. 2277–2294.

[4] B. AKGÖZ AND Ö. CIVALEK, *Buckling analysis of functionally graded microbeams based on the strain gradient theory,* Acta Mech., 224 (2013), pp. 2185–2201.

[5] V. BIRMAN, Plate Structures, Solid Mechanics and Its Applications, Vol. 178 Springer Science and Business Media, 2011.

[6] T. BOSE AND A. R. MOHANTY, *Vibration analysis of a rectangular thin isotropic plate with a part-through surface crack of arbitrary orientation and position,* J. Sound Vib., 332 (2013), pp. 7123–7141.

[7] P. K. MALLICK, Fibre-Reinforced Composites: Materials, Manufacturing and Design. Third Edition. Boca Raton, FL: CRC Press, Taylor and Francis Group, 2007.

[8] X. L. GAO AND G. Y. ZHANG, *A non-classical kirchhoff plate model incorporating microstructure, surface energy and foundation effects,* Continuum Mech. Thermodyn., 28 (1-2) (2016), pp. 195–213.

[9] A. GUPTA, N. K. JAIN, R. SALHOTRA AND P. V. JOSHI, *Effect of crack location on vibration analysis of partially cracked isotropic and fgm micro-plate with non-uniform thickness: an analytical approach,* Int. J. Mech. Sci., 145 (2018), pp. 410–429.

[10] A. GUPTA, N. K. JAIN, R. SALHOTRA AND P. V. JOSHI, *Effect of microstructure on vibration characteristics of partially cracked rectangular plates based on a modified couple stress theory,* Int. J. Mech. Sci., 100 (2015), pp. 269–282.

[11] A. GUPTA, N. K. JAIN, R. SALHOTRA, A. M. RAWANI AND P. V. JOSHI, *Effect of fibre orientation on non-linear vibration of partially cracked thin rectangular orthotropic micro plate: an analytical approach,* Int. J. Mech. Sci., 105 (2015), pp. 378–397.

[12] A. GUPTA, N. K. JAIN, R. SALHOTRA AND P. V. JOSHI, *Effect of crack location on vibration analysis of partially cracked isotropic and FGM Micro-plate with non-uniform thickness: an analytical approach,* Int. J. Mech. Sci., 145 (2018), pp. 410–429.

[13] C. S. HUANG, A. W. LEISSA AND R. S. LI, *Accurate vibration analysis of thick cracked rectangular plates,* J. Sound Vib., 330(9) (2011), pp. 2079–2093.

[14] R. ISMAIL AND M. P. CARTMELL, *An investigation into the vibration analysis of a plate with a surface crack of variable angular orientation,* J. Sound Vib., 331(12) (2012), pp. 2929–2948.

[15] A. ISRAR, M. P. CARTMELL, E. MANOACH, I. TRENDAFILOVA, W. OSTACHOWICZ, M. KRAWCZUK AND A. ZAK, *Analytical modelling and vibration analysis of cracked rectangular plates with different loading and boundary conditions,* J. Appl. Mech., 76 (2009), pp. 1–9.

[16] A. ISRAR, M. P. CARTMELL, M. KRAWCZUK, W. OSTACHOWICZ, E. MANOACH, I. TRENDAFILOVA, E. V. SHISHKINA AND PALACZ MAGDALENA, *On Approximate Analytical Solutions for Vibrations in Cracked Plates,* Appl. Mech. Mater., 5-6 (2006), pp. 315–322.

[17] M. H. JALAEI AND Ö. CIVALEK, *On dynamic instability of magnetically embedded viscoelastic porous FG nanobeam,* Int. J. Eng. Sci., 143 (2019), pp. 14–32.
[18] P. JEYARAJ, N. GANESAN AND PADMANABHAN CHANDRAMOULI, *Vibration and acoustic response of a composite plate with inherent material damping in a thermal environment,* J. Sound Vib., 320 (1-2) (2009), pp. 322–338.
[19] P. JEYARAJ, PADMANABHAN CHANDRAMOULI, AND N. GANESAN, *Vibration and acoustic response of an isotropic plate in a thermal environment,* J. Vib. Acoust., 130(5) (2008), 051005.
[20] D. K. JHA, KANT TARUN, AND R. K. SINGH, *A critical review of recent research on functionally graded plates,* Compos. Struct., 96 (2013), pp. 833–849.
[21] R. M. JONES, *Buckling of bars, plates, and shells,* J. Appl. Mech., Vol. 42, Bull Ridge Corporation, 1975.
[22] P. V. JOSHI, A. GUPTA, N. K. JAIN, R. SALHOTRA, A. M. RAWANI AND G. D. RAMTEKKAR, *Effect of thermal environment on free vibration and buckling of partially cracked isotropic and fgm micro plates based on a non classical Kirchhoff's plate theory: an analytical approach,* Int. J. Mech. Sci., (2017).
[23] P. V. JOSHI, N. K. JAIN AND G. D. RAMTEKKAR, *Analytical modeling and vibration analysis of internally cracked rectangular plates,* J. Sound Vib., 333(22) (2014), pp. 5851–5864.
[24] P. V. JOSHI, N. K. JAIN, G. D. RAMTEKKAR AND G. S. VIRDI, *Vibration and buckling analysis of partially cracked thin orthotropic rectangular plates in thermal environment,* Thin-Walled Structures, 109 (2016), pp. 143–158.
[25] P. V. JOSHI, N. K. JAIN AND G. D. RAMTEKKAR, *Analytical modelling for vibration analysis of partially cracked orthotropic rectangular plates,* Euro. J. Mech. A Solids, 50 (2015), pp. 100–111.
[26] P. V. JOSHI, N. K. JAIN AND G. D. RAMTEKKAR, *Effect of thermal environment on free vibration of cracked rectangular plate: an analytical approach,* Thin-Walled Structures, 91 (2015), pp. 38–49.
[27] S. E. KHADEM AND M. REZAEE, *Introduction of modified comparison functions for vibration analysis of a rectangular cracked plate,* J. Sound Vib., 236 (2000), pp. 245–258.
[28] KIM YOUNG-WANN, *Temperature dependent vibration analysis of functionally graded rectangular plates,* J. Sound Vib., 284 (3-5) (2005), pp. 531–549.
[29] R. B. KING, *Elastic-plastic analysis of surface flaws using a simplified line-spring model,* Eng. Fract. Mech., 18 (1983), pp. 217–231.
[30] Q. LI, V. P. IV AND K. P. KOU, *Three-dimensional vibration analysis of functionally graded material plates in thermal environment*, J. Sound Vib., 324 (3-5) (2009), pp. 733–750.
[31] K. M. LIEW, K. C. HUNG AND M. K. LIM, *A solution method for analysis of cracked plates under vibration,* Eng. Fract. Mech., 48(3) (1994), pp. 393–404.
[32] R. D. MINDLIN AND N. N. ESHEL, *On first strain-gradient theories in linear elasticity,* Int. J. Solids Struct., 4(1) (1968), pp. 109–124.
[33] D. MURPHY KEVIN AND D. FERREIRA, *Thermal buckling of rectangular plates,* Int. J. Solids Struct., 38 (2001), pp. 3979–3994.
[34] S. NATARAJAN, S. CHAKRABORTY, M. GANAPATHI AND M. SUBRAMANIAN, *A parametric study on the buckling of functionally graded material plates with internal discontinuities using the partition of unity method,* Euro. J. Mech. A Solids, 44 (2014), pp. 136–147.
[35] S. M. MOUSAVI AND J. PAAVOLA, *Analysis of plate in second strain gradient elasticity,* Arch. Appl. Mech., 84(8) (2014), pp. 1135–1143.
[36] S. PAPARGYRI-BESKOU AND D. E. BESKOS, *Static, stability and dynamic analysis of gradient elastic flexural kirchhoff plates,* Arch. Appl. Mech., 78(8) (2007), pp. 625–635.
[37] J. R. RICE AND N. LEVY, *The part-through surface crack in an elastic plate,* J. Appl. Mech., 1 (1972), pp. 185–194.

[38] Z. J. ZENG AND S. H. DAI, *Stress intensity factors for an inclined surface crack under biaxial,* Eng. Fract. Mech., 47 (1994), pp. 281–289.
[39] R. SOLECKI, *Bending vibration of a simply supported rectangular plate with a crack parallel to one edge,* Eng. Fract. Mech., 18(6) (1983), pp. 1111–1118.
[40] S. SONI, N. K. JAIN AND P. V. JOSHI, *Vibration analysis of partially cracked plate submerged in fluid,* J. Sound Vib., 412 (2018), pp. 28–57.
[41] S. SONI, N. K. JAIN AND P. V. JOSHI, *Analytical modeling for nonlinear vibration analysis of partially cracked thin magneto-electro-elastic plate coupled with fluid,* Nonlinear Dyn., 90(1) (2017), pp. 137–170.
[42] S. SONI, N. K. JAIN AND P. V. JOSHI, *Vibration and deflection analysis of thin cracked and submerged orthotropic plate under thermal environment using strain gradient theory,* Nonlinear Dyn., 96(2) (2019), pp. 1575–1604.
[43] S. SONI, N. K. JAIN, P. V. JOSHI, AND A. GUPTA, *Effect of fluid-structure interaction on vibration and deflection analysis of generally orthotropic submerged micro–plate with crack under thermal environment: an analytical approach,* J. Vib. Eng. Tech., (2019).
[44] B. STAHL, AND L. M. KEER, *Vibration and stability of cracked rectangular plates,* Int. J. Solids Structures, 8(1) (1972), pp. 69–91.
[45] R. SZILARD, Theories and Applications of Plate Analysis, Hoboken, NJ, USA: John Wiley and Sons, Inc, 2004.
[46] G. C. TSIATAS, *A new Kirchhoff plate model based on a modified couple stress theory,* Int. J. Solids Struct., 46 (13) (2009), pp. 2757–2764.
[47] K. MARUYAMA AND O. ICHINOMIYA, *Experimental study of free vibration of clamped rectangular plates with straight narrow slits,* Vib. Control Eng. Eng. Ind., 32 (1989), pp. 187–193.
[48] D. WU AND S. S. LAW, *Anisotropic damage model for an inclined crack in thick plate and sensitivity study for its detection,* Int. J. Solids Structures, 41(16-17) (2004), pp. 4321–4336.
[49] C. XU, D. RONG, Z. ZHOU, Z. DENG Z, AND C. W. LIM, *Vibration and buckling characteristics of cracked natural fiber reinforced composite plates with corner point-supports,* Eng. Structures, 214 (2020), 110614.
[50] J. YANG AND H. S. SHEN, *Vibration characteristics and transient response of shear-deformable functionally graded plates in thermal environments,* J. Sound Vib., 255(3) (2002), pp. 579–602.
[51] L. YIN, Q. QIAN, W. WANG AND W. XIA, *Vibration analysis of microscale plates based on modified couple stress theory,* Acta Mech. Solida Sinica, 23(5) (2010), pp. 386–393.